Electric Power Components and Systems

ISSN: 1532-5008 (Print) 1532-5016 (Online) Journal homepage: www.tandfonline.com/journals/uemp20

# Hilbert–Huang Transform Based Approach for Measurement of Voltage Flicker Magnitude and Frequency

Yasemin Önal, Doğan Gökhan Ece & Ömer Nezih Gerek

**To cite this article:** Yasemin Önal, Doğan Gökhan Ece & Ömer Nezih Gerek (2015) Hilbert–Huang Transform Based Approach for Measurement of Voltage Flicker Magnitude and Frequency, Electric Power Components and Systems, 43:2, 167-176, DOI: 10.1080/15325008.2014.978054

**To link to this article:** https://doi.org/10.1080/15325008.2014.978054

Published online: 31 Dec 2014.

*Electric Power Components and Systems*, 43(2):167–176, 2015

ISSN: 1532-5008 print / 1532-5016 online
DOI: 10.1080/15325008.2014.978054

# Hilbert–Huang Transform Based Approach for Measurement of Voltage Flicker Magnitude and Frequency

Yasemin Önal,[1] Doğan Gökhan Ece,[2] and Ömer Nezih Gerek[2]
[1]Department of Electric–Electronic Engineering, Bilecik Seyh Edebali University, Bilecik, Turkey
[2]Department of Electric–Electronic Engineering, Anadolu University, Eskisehir, Turkey

**CONTENTS**



**Abstract**—Voltage flicker is a non-stationary waveform for which direct spectral analysis is not appropriate. To overcome this difficulty, a Hilbert–Huang transform based technique is proposed here. Hilbert–Huang transform is a new signal processing method that can be used in the analysis of non-linear and non-stationary signals. In the suggested method, the recorded voltage signal is decomposed into Hilbert–Huang transform components, namely the empirical mode decomposition and intrinsic mode function components. These components are used in the calculation of the frequency and amplitude of voltage flicker. The clear success of empirical mode decomposition in depicting envelope variations of a sinusoidal waveform has been the main motivation for the adoption of Hilbert–Huang transform in flicker analysis. Simulations are performed over waveforms, including single- and multiple-flicker frequencies and flicker with harmonic, voltage sag, and voltage swell. The waveforms are selected as pure sinusoids, as well as harmonically rich voltage waveforms. Simulation results show that the proposed methodology constitutes a plausible way to analyze voltage flickers, making it an alternative to the available flicker analysis tools.

## 1. INTRODUCTION

Voltage flicker is a severe power quality defect that can even be visible by the human eye under electric light sources. According to the European Union EN 61000-3-3 standard, voltage flicker is described as the unstable effect of a light excitation in which brightness and spectral distribution are waves on the eye sense. The general "voltage flicker" term can be analyzed in two sub-groups, namely short-term and long-term voltage flickers. The characteristic of the voltage flicker changes based upon the type and size of the load [1]. The human eye is sensitive to voltage flicker at the 0.5- and 25-Hz frequency band. As a result, voltage flicker itself is described as voltage fluctuations between 0.5 and 25 Hz [2].

Even more important than the visibility effect is that voltage flicker is considered to be one of the harshest power quality events because of its detrimental effects on most electronic and

Keywords: voltage flicker, Hilbert–Huang transformation, empirical mode decomposition, power quality analysis
Received 17 June 2013; accepted 27 September 2014
Address correspondence to Dr. Yasemin Önal, Faculty of Engineering, Department of Electric–Electronic Engineering, Bilecik Seyh Edebali University, Bilecik, 11100, Turkey. E-mail: yasemin.onal@bilecik.edu.tr

control circuits, which are generally characterized by their sensitivity to voltage variation. The voltage flicker breaks down the operation performance of the motor and the generators, and it can cause process errors and memory losses in computers by reducing the lifespan of electronic equipment and incandescent and fluorescent lights. Voltage fluctuation can also result in the malfunction of phase-locked loops (PLLs), electronic controllers, and protection devices [3].

The gist of the flicker analysis is to determine the envelope of the voltage signal. After the envelope is determined, parameters related to flicker are calculated easily. IEC and IEEE standards suggested a way to determine the flicker envelope in [4, 5] with a method called "square demodulation," in which the square of the input voltage signal is calculated. Essentially, the above-mentioned method is a basic adoption of the well-known amplitude modulation (AM) demodulation technique used in radio communications, as explained in Section 3.

Following extraction of the envelope, several methods have been suggested in the literature for flicker quantification. In many cases, spectral strategies are adopted using fast Fourier transform (FFT). The disadvantage of applying FFT-based techniques is that in these techniques, signals are assumed as stationary [6, 7]. Other quantification methods are mostly based on estimation techniques (*e.g.*, least absolute value [LAV] status estimation and the Kalman filter [KF]). Even though LAV and KF methods are suitable for the attribution of unstable signals, these methods have essential deficiencies. The basic disadvantage of LAV-based status estimation techniques is the assumption that flicker frequency is obvious in approximation, which is not practical; furthermore, this technique suffers from slow convergence. Similarly, the KF requires a great deal of numeric calculation and accurate determination of parameters [8–11]. Recently, Hilbert transform (HT), wavelet transform (WT), and the Teager energy operator (TEO) have been used as efficient devices to analyze non-stationary waveform behavior, such as voltage flicker. In the HT technique, after the transformation of the original signal, the band-pass envelope is available for voltage flicker detection [12, 13]. In the WT technique, the voltage flicker is usually obtained from frequency region decomposition of voltage waveform [14]. A simple TEO can rapidly detect the changes in this available signal envelope; however, this method is sensitive to parasitic noise, so the accuracy deteriorates as the flicker frequency increases [15, 16].

Many classification algorithms have been developed by researchers for detection and classification of PQ disturbances, such as voltage sag, voltage swell, voltage flicker, harmonics, transients, DC components, and electromagnetic interference. The potential of a relatively recent method of ensemble empirical mode decomposition (EMD) based support vector machine (SVM) classification for analyzing non-linear and non-stationary power disturbances was applied in [17, 18]. The relatively new EMD method was proposed for the classification of power quality disturbances in [19–21]. A new noise assisted analysis method, called ensemble EMD, was proposed and its effect on time–frequency analysis behaviors investigated in [22].

Clearly, voltage flicker is a stochastic process, and its analysis remains an open issue. Inspired by the HT idea, Hilbert–Huang transform (HHT) is a new signal transformation based on decomposition of the signal into its components with instantaneous frequencies. This property is useful in the analysis of non-stationary and time-varying signals [23], making it suitable for voltage flicker detection and analysis.

In this study, an approach based on HHT is suggested to calculate the frequency and amplitude of voltage flicker. In this technique, after decomposition of the original signal through the transform, components that carry similar oscillatory characteristics are automatically bundled to the same decomposition level (known as intrinsic mode functions [IMFs]) by the EMD, enabling the envelope component to exhibit itself for voltage flicker detection. Once the flicker envelope band is detected, HT is applied to the corresponding IMF component. EMD together with HT is used for extracting mono-components (*i.e.*, the IMFs) and symmetric components from non-stationary signals. The advantages of this method are that it does not require a predetermined set of mathematical functions and that it allows projection of a non-stationary signal onto a time–frequency plane, thus making it adaptive in nature. The voltage flicker frequency, frequency error $e_{f_i}$, flicker amplitude, and amplitude error $e_{mi}$ are obtained.

This article explains the HHT method in Section 2. In Section 3, the mathematical envelope model of the voltage flicker is provided, and the motivation behind the selection of HHT for detection and analysis purposes is described. Simulation results for various cases of single- and multiple-frequency voltage flicker, harmonic flicker, voltage sag, and voltage swell signal are presented in Section 4, followed by conclusions in Section 5.

## 2. HHT METHOD

core step of the overall HHT is called the EMD, which was developed by Huang and his colleagues in 1998 [23]. This step produces the so-called IMFs that successfully correspond to separate frequency components. Inherently, the envelope oscillations of a higher frequency sinusoidal oscillation can be extracted this way, hence the detection of voltage flickers. The next step of HHT regards the quantification of these components through HT, where amplitude, instant phase, and frequency information are obtained [23].

### 2.1. EMD

EMD works by eliminating the highest frequency oscillations using subtraction of zero crossing waveform variations. In this way, the IMFs are ranked from the highest frequency to the lowest frequency. This method, therefore, decomposes the signal into zero mean AM and frequency modulation (FM) components. Every IMF symbolizes a simple oscillation in the signal. It can be thought of as a harmonic component in this respect; however, contrary to the harmonic components, the amplitude and frequencies of the IMFs are not stationary and may change in time. The EMD strategy assumes the following for a waveform:

1) the number of extreme points and the number of zero points must be equal or differ by at most one;
2) the mean of the envelope of the local maximum and the envelope of the local minimum value must be zero [16].

IMFs in EMD method are obtained as follows [23–28], considering a continuous-time signal.

1) All the maximum points of $x(t)$ are obtained and marked. An upper envelope $u(t)$ is obtained by combining upper extremum points with interpolation (typically the cubic spline [17]).
2) In the $x(t)$signal, all minimum points are obtained and marked. A lower envelope $v(t)$ is obtained by combining lower extremum points with interpolation (again, cubic spline).
3) The mean envelope $m(t)$ of the $x(t)$ signal is obtained from Eq. (1) by taking the mean of upper and lower envelopes:

$$m\left(t\right)=\left[u\left(t\right)+v\left(t\right)\right]/2 \tag{1}$$

4) A new signal $h_1(t)$ is obtained from Eq. (2) by subtracting the mean envelope from :

$$h_1(t)=x\left(t\right)-m\left(t\right) \tag{2}$$

5) If $h_1(t)$ as obtained from Eq. (2) does not satisfy IMF properties, the first four steps are applied on $h_1(t)$; this is called the *sifting* process. If the mean envelope signal satisfies the IMF properties, recursion is stopped and an (starting from the first) IMF component $c_1\left(t\right)$ is obtained. The mean signal and the mean-subtracted signal are updated as in Eq. (3):

$$\begin{aligned} m_{k-1}\left(t\right)&=\left[u_{k-1}\left(t\right)+v_{k-1}\left(t\right)\right]/2,\\ h_k\left(t\right)&=x_{k-1}\left(t\right)-m_{k-1}\left(t\right) \end{aligned} \tag{3}$$

6) The first IMF component $c_1\left(t\right)$ is subtracted from the original data, and its residue signal $r_1\left(t\right)$ is obtained from Eq. (4):

$$\begin{aligned} c_1\left(t\right)&=h_k\left(t\right),\\ r_1\left(t\right)&=x\left(t\right)-c_1\left(t\right) \end{aligned} \tag{4}$$

In the present case,  shows the highest frequency component in voltage signal. The residual signal $r_1\left(t\right)$ still has oscillatory components. Consequently, a new elimination process is started and iterated until $r_n\left(t\right)$ becomes a non-oscillating (monotonic) function. Finally, the remaining $m\left(t\right)$ signal is called a residue signal ($r_n\left(t\right)$ in Eq. (5)):

$$\begin{aligned} &r_2\left(t\right)=r_1\left(t\right)-c_2\left(t\right),r_3\left(t\right)=r_2\left(t\right)-c_3\left(t\right),\ldots,\\ &r_n(t)=r_{n-1}\left(t\right)-c_n\left(t\right). \end{aligned} \tag{5}$$

Clearly, the original signal can be reconstructed as the sum of IMF components and the last residual mean as in Eq. (6):

$$x\left(t\right)=r_n\left(t\right)+\sum_{j=1}^{n}c_j\left(t\right) \tag{6}$$

As indicated above, once the IMFs are obtained, they may be used to estimate the characteristics of the local frequencies in the signal.

### 2.2. HT

HT is applied to the IMF components as a result of EMD, and the Hilbert spectrum is obtained. After HT is applied to every IMF component $c_j\left(t\right)$, a new data serial $y_j\left(t\right)$ is obtained from Eq. (7):

$$y_t(t)=\frac{1}{\pi}P\left\{\int_{-\infty}^{\infty}\frac{C_j(t)}{t-\tau}d\tau\right\}, \tag{7}$$

where $P$ shows the Cauchy principle value. A complex data serial in Eq. (8) is made up from this description:

$$z_j\left(t\right)=c_j\left(t\right)+i\cdot y_j\left(t\right)=a_j\left(t\right)e^{i\theta_j(t)} \tag{8}$$

From Eq. (8), amplitude is obtained from Eq. (9):

$$\begin{aligned} a_j\left(t\right)&=\sqrt{c_j^2\left(t\right)+y_j^2\left(t\right)},\\ \theta_j\left(t\right)&=\tan^{-1}\left\{\frac{y_j\left(t\right)}{c_j\left(t\right)}\right\}, \end{aligned} \tag{9}$$

and instant frequency is calculated as $\omega_j\left(t\right)=\frac{d\theta_j(t)}{dt}$. The resultant $a_j\left(t\right)$ and $\omega_j(t)$ values are varying as a function of time. The overall algorithm layout is shown in Figure 1.

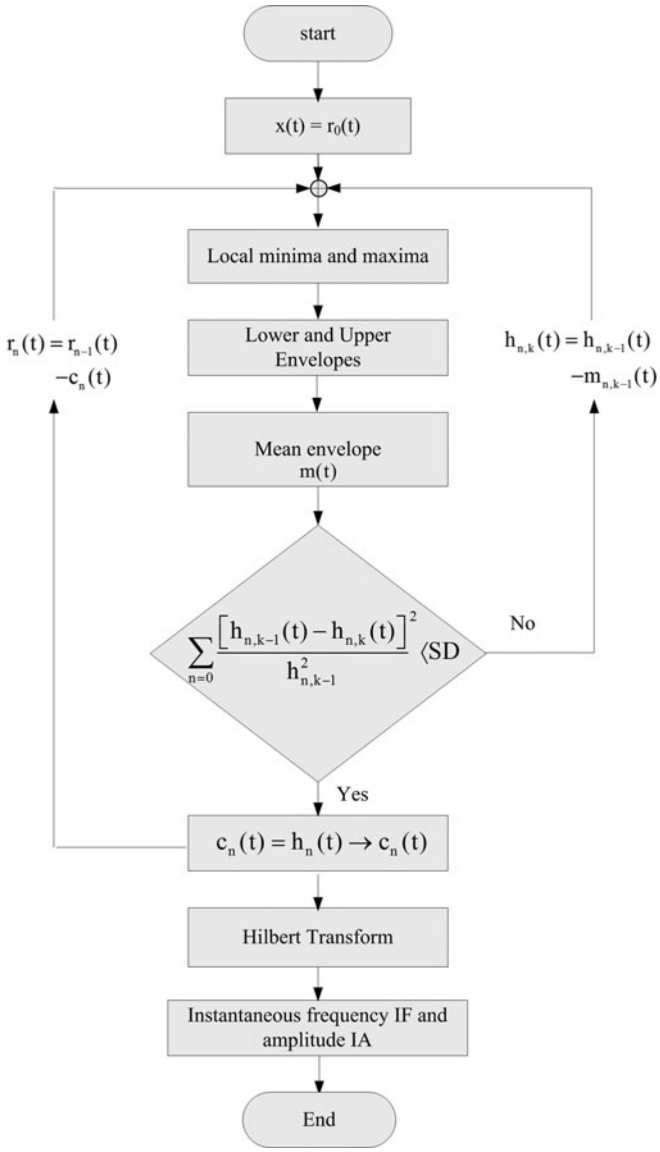


**FIGURE 1.** HHT algorithm.

## 3. HHT OF VOLTAGE FLICKER

### 3.1. Mathematical Model of Voltage Flicker

Accurate extraction of the voltage flicker component is the desired output of the proposed model. Naturally, voltage flicker waveform can be modeled as adding AM (envelope) harmonic components to the sinusoidal waveform. Due to telecommunications, this model can be expressed as in Eq. (10) [29]:

$$
\begin{aligned}
u(t) &= A_0 \left[1 + \sum_{i=1}^{N} m_i \cos(2\pi f_i t + \phi_i)\right] \cos(2\pi f_0 t + \varphi_0),\\
&= [A_0 + A_0 v(t)] \cos(2\pi f_0 t + \varphi_0),\\
&= A(t) \cos(2\pi f_0 t + \varphi_0). \qquad (10)
\end{aligned}
$$

In Eq. (10), $A_0$ is the amplitude of the main signal, $f_0$ is the main frequency, $\varphi_0$ is the elementary phase angle, $m_i$ is the ratio of the flicker amplitude to the main amplitude, and $f_i$ and $\phi_i$ are the frequency of flicker voltage and elementary phase angle, respectively. Here, $A_0 v(t) = A_0 \sum_{i=1}^{h} m_i \cos(2\pi f_i t + \phi_i)$ corresponds to the flicker envelope.

### 3.2. Acquiring the Flicker Envelope

The simplest AM demodulation algorithm is the square-law detector (used in many AM radios, also adopted by flicker detection standards). If the square of $u(t)$ (in Eq. (10)) is taken, the output is

$$
\begin{aligned}
u^2(t) = &\left(\frac{A_0^2 + A_0^2 \cos(2\pi(2f_0)t + \varphi_0)}{2}\right)\\
&\times\Bigg[1 + \sum_{i=1}^{N} m_i^2 \cos^2(2\pi f_i t + \phi_i)\\
&+2\sum_{i=1}^{N}\sum_{j=i+1}^{N} m_i m_j \cos(2\pi f_i t + \phi_i)\cos\\
&\times(2\pi f_{ij} t + \phi_{ij}) +\\
&2\sum_{i=1}^{N} m_i \cos\left(2\pi f_i t + \phi_i\right)\Bigg]\\
= &\frac{A_0^2}{2} + A_0^2 \sum_{i=1}^{N} m_i \cos(2\pi f_i t + \phi_i) + A_0^2 \cos\big(2\pi(2f_0)t\\
&+\varphi_0\big) \sum_{i=1}^{N} m_i \cos\left(2\pi f_i t + \phi_i\right)\\
&+\left(\frac{A_0^2}{2} + \frac{A_0^2}{2}\cos(2\pi(2f_0)t + \varphi_0)\right)\\
&\sum_{i=1}^{N} m_i^2 \cos^2(2\pi f_i t + \phi_i) + \frac{A_0^2}{2}\\
&\times \cos(2\pi(2f_0)t + \varphi_0)\\
&+\left(A_0^2 + \frac{A_0^2}{2}\cos(2\pi(2f_0)t + \varphi_0)\right)\sum_{i=1}^{N}\sum_{j=i+1}^{N} m_i m_j\\
&\times \cos(2\pi f_i t + \phi_i)\cos(2\pi f_j t + \phi_j). \qquad (11)
\end{aligned}
$$

In Eq. (11), since $m \ll 1$, the terms that multiply $m_i^2$ and $m_i m_j$ can be safely ignored to achieve an approximation:

$$
\begin{aligned}
u^2(t) \cong &\frac{A_0^2}{2} + A_0^2 \cos(2\pi(2f_0)t + \varphi_0) \sum_{i=1}^{N} m_i \cos(2\pi f_i t + \phi_i)\\
&+\frac{A_0^2}{2}\cos(2\pi(2f_0)t + \varphi_0)\\
&+A_0^2 \sum_{i=1}^{N} m_i \cos(2\pi f_i t + \phi_i). \qquad (12)
\end{aligned}
$$

It can be noticed that the flicker envelope $A_0^2 \sum_{i=1}^{N} m_i \cos(2\pi f_i t + \phi_i)$ is eminent in Eq. (12). The other terms are additive components at frequencies more than twice the fundamental line frequency (which is already expected to be way more than the flicker frequency components); they can therefore be filtered out using a low-pass filter. After acquiring the envelope, HT or other spectral techniques can be used to determine the flicker parameters.

This standard methodology has some important drawbacks:

- if the flicker component envelopes ($m_j$) are relatively large, the square-law approximation in Eq. (12) becomes inaccurate, causing inaccurate magnitude and frequency calculations in the forthcoming steps;
- as the flicker frequency increases (approaching line frequency $m_j$), low-pass filtering may become impossible; and
- the method is not able to resolve harmonic components of the envelope.

The HHT approach that starts by EMD yields nice remedies to these drawbacks. Due to the voltage flicker waveform is modeled as amplitude modulated, and the number of extreme points of voltage flicker waveform is equal to the number of zero-crossing points. The square of the voltage flicker waveform is obtained before applying EMD to break the symmetry (+/– is equal in terms). Quite simply, the highest frequency IMF corresponds to the line frequency (fundamental) component, regardless of the flicker envelope magnitude. Therefore, the accuracy of the later quantification process is assured. Furthermore, the method does not require any linear low-pass filtering; therefore, frequency mixture is significantly less in the HHT technique. Finally, The EMD step automatically decomposes the flicker into its harmonic components for more accurate flicker quantification and analysis.

## 4. SIMULATIONS

Simulations are performed in MATLAB (The MathWorks, Natick, Massachusetts, USA). The flicker-contaminated data were obtained by digitizing a three-phase, 30-kVA programmable disturbance generator (BPS-30-1/3 30 kVA; California Instruments), which was fed by waveform files. The waveform files contain comma separated value (CSV) data that contain pure sinusoids added by flicker envelopes at various frequency and amplitudes.

Single frequency, multiple frequency, harmonic flicker signal, voltage sag, and swell signal are tested for the above-mentioned method. For all identified samples, the amplitude of the voltage signal is normalized to unity. Voltage waveform sampling frequency is taken as 10 kHz. Clearly, a sampling frequency above the Nyquist rate is necessary to contain all of the necessary information of the analog signal. In the present case, the flicker is a sub-harmonic with a frequency lower than 50 Hz. However, the transient waveform may contain non-sinusoidal shapes, which naturally contain a much higher frequency content. To capture all subtle envelope shape variations and take their effects into account, a high sampling rate of 10 kHz is chosen. It was experimentally observed that the numerical results do not change for higher sampling rates; however, the possibly sharper flicker envelopes were not faithfully reconstructed with sampling rates below 5 kHz. The ratio of flicker amplitude to the amplitude of the source signal $m_i$ is called the flicker amplitude. After acquiring the flicker envelope, its quantification is performed over four components: flicker frequency $f_i$ (Hz), frequency error $e_{fi}$ (%), flicker amplitude $m_i$ (p.u.), and amplitude error $e_{mi}$ (%). Voltage waveform sampling frequency is taken as 10 kHz. The flicker frequencies and amplitudes have been set according to the voltage fluctuation values given in flickermeter standard 61000-4-15.

### 4.1. Single-frequency Voltage Flicker

The expression of voltage, which was modulated with single flicker, is shown in Eq. (13):

$$u(t) = A_0[1 + m\cos(2\pi f t + \phi_1)]\cos(2\pi f_0 t + \varphi_0) \quad (13)$$

Here, the parameters are chosen as $A_0 = 1$, $m = 0.176$, $f = 8.8$ Hz, $\phi_1 = 0$, $f_0 = 50$ Hz, and $\varphi_0 = 0$ [13]. Following EMD, the flicker signal component IMF is obtained as shown in Figure 2(a). HT is applied to this IMF to obtain flicker frequency and amplitude. The results are illustrated in Figures 2(b) and 2(c), respectively. Naturally, HT provides a time function for the flicker amplitude. Since the applied flicker amplitude does not change in time, the measurement is done by taking the mean (average) value of the output, and the result obtained is 0.175992. The percentage error of this amplitude is a mere 0.004204%. With a similar strategy, the flicker frequency is obtained as 8.79901 Hz, which corresponds to a relative error of 0.007940%. The results are also presented in tabular form in Table 1 [30]. For all practical purposes, the method successfully identifies single-frequency voltage flicker.

According to [4], flicker frequencies over 25 Hz have negligible effects. The practical range of parameters according to [29] is indicated as flicker amplitude ($m_i$) between 1% and 10% and flicker frequency ($f_i$) between 3.5 and 24 Hz. For comparative purposes, the outputs of the proposed method are presented in Tables 2 and 3.

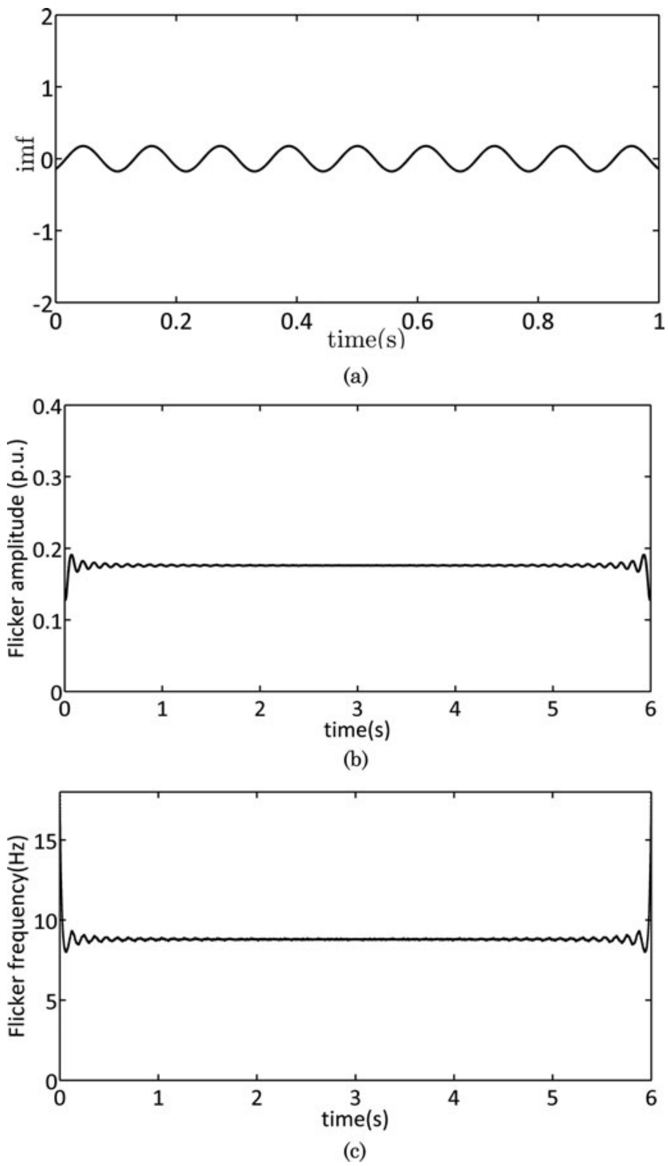


**FIGURE 2.** HHT analysis of single-frequency voltage flicker.

It can be seen that both the frequency and amplitude values of the recovered flicker signals are within reasonable bounds throughout the useful range.

The voltage signal with single-frequency flicker is measured by using the HHT and square demodulation methods. To make a realistic simulation analysis, flicker frequency $f$ and amplitude $m$ are set according to voltage fluctuation values of instantaneous flicker level (IFL) [4]. As defined in IEC 61000-4-15, if input values are within the ±5% limits of values in the table for a unit output of perceptibility, the desired accuracy is obtained. The comparison of the two methods are shown in Figure 3. It is seen that HHT-based methods give more accurate results than square demodulation (SD) methods.

| Parameter | $f$ (Hz) | $m$ (p.u.) |
|---|---|---|
| Setting value | 8.800000 | 0.176000 |
| Measurement value | 8.799301 | 0.175992 |
| Error (%) | 0.007940 | 0.004204 |

**TABLE 1.** Flicker signal amplitude and frequency

| Setting value | Measurement value | | | |
|---|---|---|---|---|
| $f_i$ (Hz) | $f_i$ (Hz) | efi (p.u.) | mi (p.u.) | emi (p.u.) |
| 3.5 | 3.4999582 | 0.0011946 | 0.0200005 | –0.0018258 |
| 4.5 | 4.4999768 | 0.0005163 | 0.0200001 | 0.0001728 |
| 5.5 | 5.4999352 | 0.0011782 | 0.0200001 | 0.0000790 |
| 6.5 | 6.4998521 | 0.0022757 | 0.0200001 | 0.0001957 |
| 7.5 | 7.4997465 | 0.0033798 | 0.0199998 | 0.0016914 |
| 8.8 | 8.7996105 | 0.0044267 | 0.0200000 | 0.0001545 |
| 10.0 | 10.0005916 | –0.0059158 | 0.0200000 | 0.0007141 |
| 15.0 | 14.9979269 | 0.0138227 | 0.0199931 | 0.0354112 |
| 20.0 | 20.0051404 | –0.0256953 | 0.0199997 | 0.0022122 |
| 24.0 | 24.0062344 | –0.0259700 | 0.0199924 | 0.0387975 |

**TABLE 2.** Result of $m_i = 0.02$ p.u. with single frequency

After flicker envelope is obtained using two methods, the IFL is obtained. The IFL errors (%) obtained from the test results are compared in Figure 4.

### 4.2. Multi-frequency Voltage Flicker

The expression of the flicker-contaminated voltage with two flicker frequency components is given in Eq. (14):

$$u(t) = A_0[1 + m_1 \cos(2\pi f_1 t + \phi_1) + m_2 \cos(2\pi f_2 t + \phi_2)] \times \cos(2\pi f_0 t + \varphi_0) \tag{14}$$

| Setting value | Measurement value | | | |
|---|---|---|---|---|
| $f_i$ ($Hz$) | $f_i$ (Hz) | $e_{fi}$ (p.u.) | $m_i$ (p.u.) | $e_{mi}$ (p.u.) |
| 3.5 | 3.4999802 | 0.0005650 | 0.0600002 | –0.0000450 |
| 4.5 | 4.4999385 | 0.0013659 | 0.0600000 | 0.0001862 |
| 5.5 | 5.4999197 | 0.0014608 | 0.0600001 | 0.0000867 |
| 6.5 | 6.4998499 | 0.0023097 | 0.0600000 | 0.0001693 |
| 7.5 | 7.4997475 | 0.0033669 | 0.0599991 | 0.0016909 |
| 8.8 | 8.7996101 | 0.0044310 | 0.0599995 | 0.0009915 |
| 10.0 | 10.0005916 | –0.0059158 | 0.0599997 | 0.0007141 |
| 15.0 | 14.9987363 | 0.0084255 | 0.0599941 | 0.0101109 |
| 20.0 | 20.0006977 | –0.0034883 | 0.0600001 | –0.0113954 |
| 24.0 | 24.0063440 | –0.0264265 | 0.0600001 | 0.0498357 |

**TABLE 3.** Result of $m_i = 0.06$ p.u. with single frequency

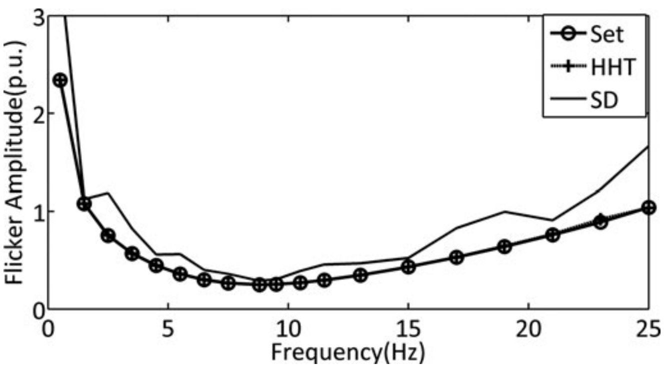


**FIGURE 3.** Comparison of applied values, HHT values, and SD values.

In Eq. (14) the parameters are chosen as $A_0 = 1$, $m_1 = 0.00141$, $f_1 = 5$ Hz, $\phi_1 = 0$, $m_2 = 0.00153$, $f_2 = 15$ Hz, $\phi_2 = 0$, $f_0 = 50$ Hz, and $\varphi_0 = 0$. Two flicker components are acquired as a result of EMD: $\text{IMF}_1$ and $\text{IMF}_2$. $\text{IMF}_1$ exhibits the component with higher frequency and $\text{IMF}_2$ the component with lower frequency. Similar to the above analysis, HT is applied to the $\text{IMF}_1$ and $\text{IMF}_2$ signals to obtain the frequencies and amplitudes of these flicker components. Amplitudes (as a function of time) of the flicker components are shown in Figures 5(a) and 5(b). The mean value of the amplitude of the first flicker component is 0.0014056. When the amplitude value is compared with the applied value, the error is 0.1102016%. The mean value of the amplitude of the second component of the flicker signal is 0.0015248, with a relative error of 0.1652988%. Frequencies of the flicker components are presented in Figures 5(c) and 5(d). The mean value of the frequency of the first flicker component is 4.9991634 Hz with a relative error of 0.0167353%, and the mean value of the frequency of the second flicker component is 14.9996616 with a relative error of 0.0022563%.

In Table 4, HHT, TEO, and SD methods are compared; it can be seen that frequency error and amplitude error values calculated using HHT are below 0.16%. The frequency error and amplitude error values calculated with other methods (TEO and SD) are comparably higher than HHT. When the HHT, TEO, and SD methods are compared, it is seen that HHT method gives more accurate results. Again, the retained values are well within a tolerable error bound.

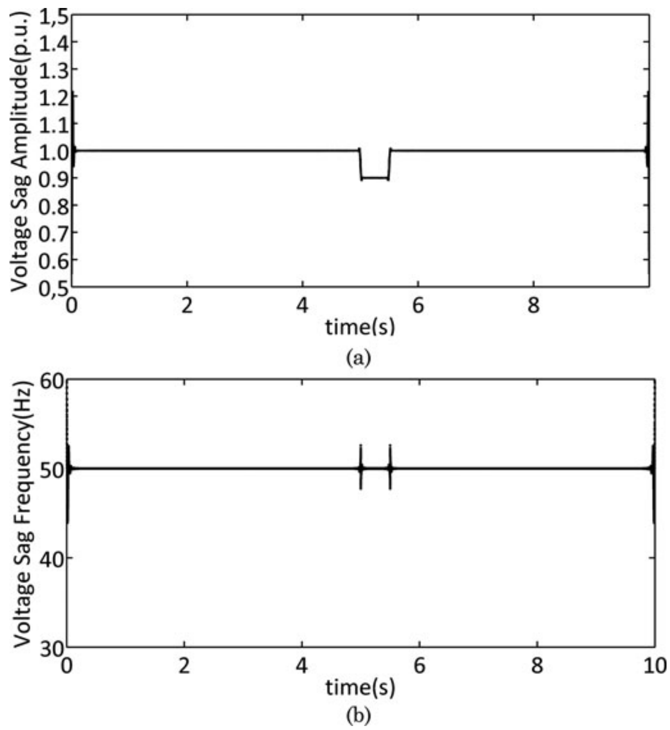


**FIGURE 5.** HHT analysis of voltage flicker with harmonics.

## 4.3. Voltage Flickers under Harmonically Rich Voltage Waveforms

The overall expression of a voltage waveform, which includes harmonic components as well as a flicker, is given in Eq. (15):

$$u(t) = A_0[1 + m\cos(2\pi f_1 t + \phi_1)]\cos(2\pi f_0 t + \varphi_0) + \sum_{i=3,5} A_i \cos(2\pi m_i f_0 t + \varphi_0) \tag{15}$$

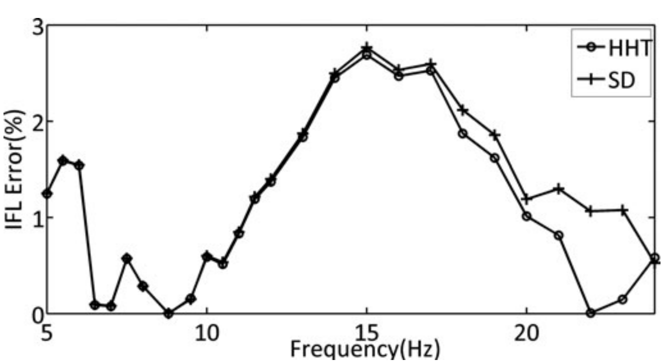


**FIGURE 4.** Comparison of IFL error of HHT and SD values.

| | | |
|---|---|---|
| Setting frequency (Hz) | 5 | 15 |
| Setting amplitude (p.u.) | 0.00141 | 0.00153 |
| HHT frequency (Hz) | 4.9991634 | 14.9996616 |
| HHT frequency error (%) | 0.0167353 | 0.0022563 |
| HHT amplitude (p.u.) | 0.0014056 | 0.0015248 |
| HHT amplitude error (%) | 0.1102016 | 0.1652988 |
| TEO amplitude (p.u.) | 0.0014045 | 0.0015445 |
| TEO amplitude error (%) | 0.394 | 0.945 |
| SD amplitude (p.u.) | 0.0013842 | 0.0015425 |
| SD amplitude error (%) | 1.828 | 0.819 |

**TABLE 4.** Results of multi-frequency voltage signals

In Eq. (15), the parameters are chosen as $A_0 = 1$, $m = 0.1$, $f_1 = 3$ Hz, $\phi_1 = 0$, $f_0 = 50$ Hz, $\varphi_0 = 0$, $A_3 = 0.05$, $A_5 = 0.03$, $m_3 = 3$, $m_5 = 5$, $m_3 * f_0 = 150$ Hz, and $m_5 * f_0 = 250$ Hz [18]. Again, HT is applied to the IMF component, and flicker frequency and amplitude are obtained. The results are shown in Figures 5(a) and 5(b), respectively. The mean value of the flicker amplitude is 0.1020 with a relative error corresponding to 2.0212%. The mean value of the flicker frequency is 2.9999 Hz, which corresponds to a relative error of 0.0027%.

Despite the confusing effect of harmonics within the line voltage (without the flicker), the flicker component is observed to be accurately extracted by the proposed HHT method.

### 4.4. Voltage Sag and Voltage Swell Waveforms

The overall expression of a voltage sag waveform, which includes voltage sag in Eq.16:

$$u(t) = 1\cos(2\pi f_0 t + \varphi_0)\begin{Bmatrix} 0 \le t \le 5 \\ 5.5 \le t \le 10 \end{Bmatrix}, \tag{16}$$

$$u(t) = 0.9\cos(2\pi f_0 t + \varphi_0)\{5 \le t \le 5.5\}.$$

In Eq. (16), the parameters are chosen as follows: amplitude is 1 p.u. if $t$ is between $0 \le t \le 5$ and $5.5 \le t \le 10$, other amplitude is 0.9 p.u., $f_0 = 50$ Hz, and $\varphi_0 = 0$. Again, HT is applied to the $\text{IMF}_1$ component, and voltage sag frequency and amplitude are obtained. The results are shown in Figures 6(a) and 6(b), respectively.

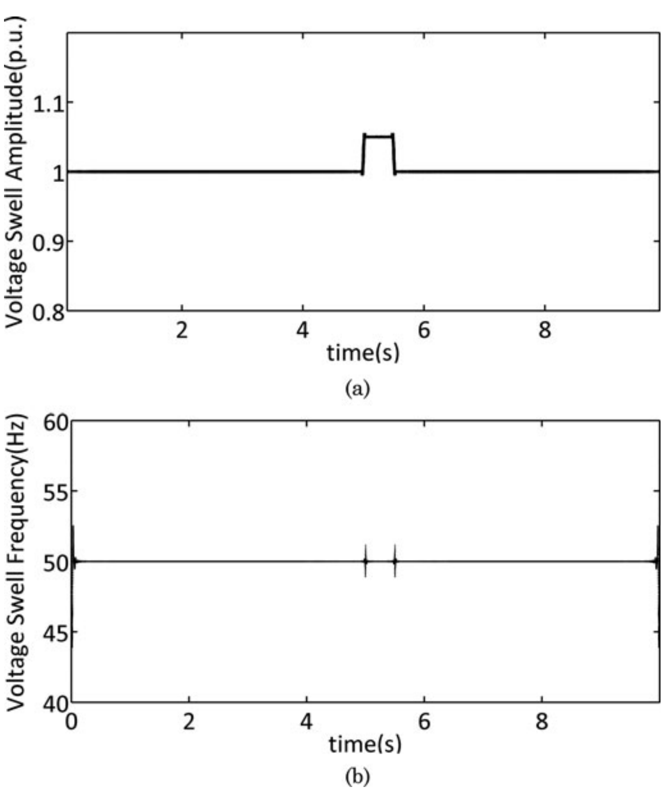


**FIGURE 6.** HHT analysis of voltage sag signal.

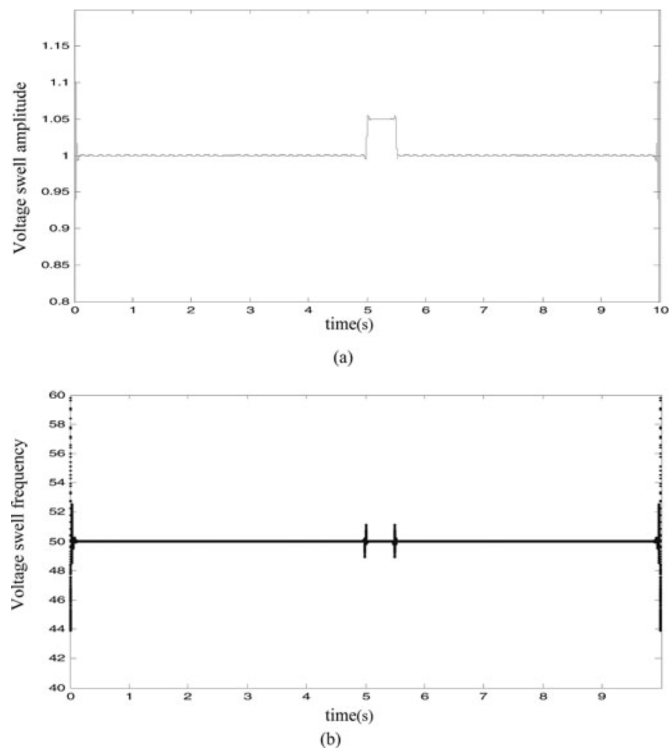


**FIGURE 7.** HHT analysis of voltage swell signal.

The overall expression of a voltage swell waveform, including voltage sag, is given in Eq. (17):

$$u(t) = 1\cos(2\pi f_0 t + \varphi_0)\begin{Bmatrix} 0 \le t \le 5 \\ 5.5 \le t \le 10 \end{Bmatrix}, \tag{17}$$

$$u(t) = 1.05\cos(2\pi f_0 t + \varphi_0)\{5 \le t \le 5.5\}.$$

In Eq. (17), the parameters are chosen as follows: amplitude is 1 p.u. if $t$ is between $0 \le t \le 5$ and $5.5 \le t \le 10$, other amplitude is 1.05 p.u., $f_0 = 50$ Hz, and $\varphi_0 = 0$. Again, HT is applied to the $\text{IMF}_1$ component, and voltage swell frequency and amplitude are obtained. The results are shown in Figures 7(a) and 7(b), respectively.

## 5. CONCLUSIONS

HHT is a novel technique that is capable of splitting signal components with different spectral characteristics. Despite this capability, it was not applied to the analysis of voltage flicker under various parametric conditions. The simulation results indicate that this method has the following pronounced advantages over existing methods.

1. The method is able to determine frequency and amplitude parametrers of the flicker with extreme accuracy within the parametric range of interest.
2. The method is capable of isolating separate flicker components, which gives a great advantage to quantification, unlike the classical square-law demodulation strategy.
3. Even under cases with normal voltage carrying harmonics, the flicker component could be extracted and accurately measured.
4. Naturally, once the amplitude and frequencies are accurately measured, short-term flicker severity ($P_{st}$) may be achieved easily.

## REFERENCES


[1] IEC, "Electromagnetic compatibility (EMC)—Part 3-3: Limitation of voltage fluctuations and flicker in low-voltage supply systems for equipment with rated current ≤16 A," IEC Standard 1000-3-3, *CENELEC*, 1994.

[2] Kennedy, B. W., "Power quality characteristics," in *Power Quality Primer*, New York: McGraw-Hill Companies, 2000.

[3] Gunther, E. W., "Interharmonics in power systems," *Power Eng. Soc. Summer Mtg.*, Vol. 2, pp. 813–817, 2001.

[4] IEC, "Flickermeter: Functional and design specifications," *IEC Standard* 61000-4-15, 1999.

[5] IEEE, "IEEE recommended practice for measurement and limits of voltage fluctuations and associated light flicker on AC power systems," IEEE Standard 1453, 2004.

[6] Srinivasan, K., "Digital measurement of voltage flicker," *IEEE Trans. Power Deliv.*, Vol. 6, No. 4, pp. 1593–1598, October 1991.

[7] Toivonen, L., and Mörsky, J., "Digital multirate algorithms for measurement of voltage, current, power and flicker," *IEEE Trans. Power Deliv.*, Vol. 10, No. 1, pp. 116–126, January 1995.

[8] Girgis, A. A., Stephens, J. W., and Makram, E. B., "Measurement and prediction of voltage flicker magnitude and frequency," *IEEE Trans. Power Deliv.*, Vol. 10, pp. 1600–1605, July 1995.

[9] Köse, N., Solar, Ö., and Leblebicioğlu, K., "A Kalman filtering based approach for light flicker evaluation of power systems," *IET Generat. Transm. Distribut.*, Vol. 2, pp. 57–69, 2011.

[10] Girgis, A. A., and Markam, E. B., "Measurement of voltage flicker magnitude and frequency using a Kalman filtering based approach," *Proc. IEEE Can. Conf. Elect. Comput. Eng.*, Vol. 2, pp. 659–662, 1996.

[11] Abdel-Galil, T. K., El- Saadany, E. F., and Salama, M. A., "Online tracking of voltage flicker utilizing energy operator and Hilbert transform," *IEEE Trans. Power Deliv.*, Vol. 19, No. 2, pp. 861–867, April 2004.

[12] Marei, M. I., Abdel-Galil, T. K., El-Saadany, E. F., and Salama, M. A., "Hilbert transform based control algorithm of the DG interface for voltage flicker mitigation," *IEEE Trans. Power Deliv.*, Vol. 20, No. 2, pp. 1129–1133, 2005.

[13] Xiaopu, W., Yonghai, X., and Xiangning, X., "Parameter estimation of voltage flicker based on Hilbert transform and pisarenko harmonic decomposition," *International Conference on Energy and Environment Technology*, pp. 189–192, Guilin, Guangzi, 16–18 October 2009.

[14] Zhang, R., and Xu, J. F., "The application of wavelet in the short-term flicker severity calculation," *2008 International Symposium on Information Science and Engineering*, pp. 511–514, Shanghai, 20–22 December 2008.

[15] Chen, Q., Jia, X., and Zhao, C., "Analysis on measuring performance of three flicker detecting methods," *Power Energy Society General Meeting*, pp. 1–7, Calgary, AB, 26–30 July 2009.

[16] Shu, H., and Wang, Y., "Detection of voltage flicker based on mathematical morphology filter and Teager energy operator," *International Conference on Power System Technology*, pp. 1–6, Chongqing, 22–26 October 2006.

[17] Yalcin, T., Ozgonenel, O., and Kurt, U., "Multi-class power quality disturbances classification by using ensemble empirical mode decomposition based SVM," *IEEE 2011 Electrical and Electronics Engineering*, pp. I-122–I-126, Bursa, Turkey, 1–4 December 2011.

[18] Ozgonenel, O., Yalcin, T., Guney, I., and Kurt, U., "A new classification for power quality events in distribution system," *Elect. Power Syst. Res.*, Vol. 95, pp. 192–199.

[19] Yalcin, T., Ozgonenel, O., and Kurt, U., "Feature vector extraction by using empirical mode decomposition for power quality disturbances," *IEEE 2011 Environment and Electrical Engineering*, pp. 1–4, Rome, 8–11 May 2011.

[20] Yun, L. T., Yan, Z., Qiang, Y., and Jian Bo, Z., "Application of emprical Hilbert Huang transform method in detection of harmonic and voltage flicker," *Power Syst. Technol.*, Vol. 29, No. 2, pp. 73–77, 2005.

[21] Hui, J., Xiaoqiang, W., and Jianchun, P., "Method to measure voltage flicker based on Hilbert-Huang transform," *Power Syst. Technol.*, Vol. 36, No. 9, pp. 256–259, 2012.

[22] Wang, T., Zhang, M., Yu, Q., and Zhang, H., "Comparing the applications of EMD and EEMD on time frequency analysis of seismic signal," *J. Appl. Geophys.*, Vol. 83, pp. 29–34, 2012.

[23] Huang, N. E., Shen, Z., Long, S. R., Wu, M. C., Shih, H. H., Zheng, Q., Yen, N.-C., Tung, C. C., and Liu, H. H., "The emprical mode decomposition and the Hilbert spectrum for nonlinear and non-stationary time series analysis," *Proc R. Soc. Lond A.*, vol. 454, pp. 903–905, 1998.

[24] Rilling, G., Flandrin, P., and Gonvalves, P., "On emprical mode decomposition and its algorithms," *EEE-EURASIP Workshop on Nonlinear Signal and Image Processing (NSIP-03)*, Grado, Italy, June 2003.

[25] Liu, W., Huang, C., Xing, Y., and Wu, Y., "Application of emprical mode decomposition and Hilbert spectrum analysis on detection of voltage flicker," *Comput. Measur. Control*, Vol. 14, No. 6, pp. 707–756, 2006.

[26] Yang, C., Dong, S., Tong, Z., and Wan, Y., "Analysis and research of the transient composite disturbance signal of power system based on HHT," *International Symposium on Intelligent Information Technology Application Workshops*, pp. 1029–1032, Shanghai, 21–22 December 2008.

[27] Yu, J., and Yang, L., "Analysis of harmonic and inter-harmonic based on Hilbert Huang transform," *International Conference*

*on Computational Intelligence and Software Engineering*, pp. 1–4, Wuhan, 11–13 December 2009.

[28] Baykut, S., Akgül, T., and Ergintav, S., "EMD based analysis and denoising of GPS data," *IEEE 17th Signal Processing and Communications Applications Conference (SIU 2009)*, pp. 644–647, Antalya, 9–11 April 2009.

[29] Jia, X., and Chen, Q., "A method of tracking voltage flicker envelope real-time," *IEEE Power & Energy Society General Meeting (PES'09)*, pp. 1–6, Calgary, AB, 26–30 July 2009.

[30] Önal, Y., Ece, D. G., and Gerek, Ö. N., "Analysis of voltage flicker using Hilbert-Huang transform," *19th IEEE Conference on Signal Processing and Communications Applications*, Kemer Antalya, Turkey, 20–22 April 2011.

## BIOGRAPHIES

**Yasemin Önal** was born in Giresun, Turkey, in 1976. She received her electrical teacher degree from Kocaeli University in 2000 and her Ph.D. from the Electrical and Electronics Engineering Department, Anadolu University, Eskisehir, Turkey, in 2011. She is currently an assistant professor in the Electrical and Electronics Engineering Department, Bilecik Seyh Edebali University, Bilecik, Turkey. Her research areas include power quality analsis and signal processing.

**Doğan Gökhan Ece** was born in Ankara, Turkey, in 1964. He received his engineering degree from Istanbul Technical University in 1986 and his M.Sc.and Ph.D. from Vanderbilt University, Nashville, TN, 1990 and 1993, respectively, all in electrical engineering. Currently he is a professor in the Electrical and Electronics Engineering Department in Anadolu University, Eskisehir, Turkey. His research areas include power quality, fault detection, and modeling.

**Ömer Nezih Gerek** received his B.Sc., M.Sc., and Ph.D. in electrical engineering from Bilkent University, Ankara, Turkey, in 1991, 1993, and 1998, respectively. During his Ph.D. studies, he spent a semester at the University of Minnesota, Minnesota, USA, as an exchange researcher. Following his Ph.D., he spent one year as a research associate at École Polytechnique Fédérale de Lausanne (EPFL) Lausanne, Switzerland. He is currently a full professor of electrical engineering at Anadolu University, Eskisehir, Turkey. He is on the editorial board of the *Turkish Journal of Electrical Engineering and Computer Science* and Elsevier's *Digital Signal Processing*. He is a member of the Electrical, Electronics and Informatics Research Fund Group of the Scientific and Technological Research Council of Turkey. His current research interests include signal processing and analysis.